Energy distributions of H^+ fragments ejected by fast proton and electron projectiles in collision with H_2O molecules

A. L. F. de Barros,[1] J. Lecointre,[2] H. Luna,[3] M. B. Shah,[4] and E. C. Montenegro[3,*]
[1]*Departamento de Ensino Superior, Centro Federal de Educação Tecnológica Celso Suckow da Fonseca, Avenida Maracanã 229, Rio de Janeiro 20271-110, RJ, Brazil*
[2]*Department of Chemistry, Durham University, South Road, Durham DH1 3LE, United Kingdom*
[3]*Instituto de Física, Universidade Federal do Rio de Janeiro, Caixa Postal 68528, Rio de Janeiro 21945-970, RJ, Brazil*
[4]*Department of Pure and Applied Physics, The Queen's University of Belfast, Belfast BT7 1NN, United Kingdom*
(Received 18 March 2009; published 31 July 2009)

Experimental measurements of the kinetic energy distribution spectra of H^+ fragment ions released during radiolysis of water molecules in collision with 20, 50, and 100 keV proton projectiles and 35, 200, 400, and 1000 eV electron projectiles are reported using a pulsed beam and drift tube time-of-flight based velocity measuring technique. The spectra show that H^+ fragments carrying a substantial amount of energy are released, some having energies well in excess of 20 eV. The majority of the ions lie within the 0–5 eV energy range with the proton spectra showing an almost constant profile between 1.5 and 5 eV and, below this, increasing gradually with decreasing ejection energy up to the near zero energy value while the electron spectra, in contrast, show a broad maximum between 1 and 3 eV and a pronounced dip around 0.25 eV. Beyond 5 eV, both projectile spectra show a decreasing profile with the electron spectra decreasing far more rapidly than the proton spectra. Our measured spectra thus indicate that major differences are present in the collision dynamics between the proton and the electron projectiles interacting with gas phase water molecules.

DOI: 10.1103/PhysRevA.80.012716 PACS number(s): 34.50.Gb, 52.20.Hv, 34.80.Ht, 52.20.Fs

I. INTRODUCTION

The dissociation pathways and the energy releases of fragments ejected from water molecules excited to high lying electronic repulsive states in collision with energetic projectiles still remain little understood despite abundant presence of such processes in important areas of physics, biology, and chemistry. The various repulsive precursor states populated are greatly dependent on whether the collision involves ionization or, in the case of protons, a capture of an electron as well, whether a removal of one or more target electron is involved, and on how efficiently a projectile is able to transfer the required amount of energy needed to populate the repulsive states. These are complex questions that cannot be reliably answered from the theoretical prospective and experimental measurements are the only resorts presently available to provide the needed data to the physics, the medicine, and the chemistry communities. Accurate information on the dissociation pathways and the energy releases are of fundamental importance in the testing and the improving of current models of radiolysis particularly those related to water loss on comet and planetary atmospheres and in the x-ray and the proton based cancer therapies where DNA morbidity through chemistry with water radicals plays a central role [1]. They are also of great importance in characterizing the evolving wave functions and the potential energy surfaces of excited water, a task currently undertaken by the theoretical chemistry community [2].

It is only in recent years that the measurements of collision induced fragmentation of water have received more attention. Measurements have been carried out on cross sections of the fragmented products by H^+ ions [3], by H^+ and He^+ ions [4,5], and by heavy multiply charged ions [6]. For electron impact the measurements are rather limited as well and available measurements show significant disagreements with one another (see, for instance, [7] and, more recently, [8]). The measurements of the energy distribution of the fragments released are even more limited. For heavy ions, the measurements by H^+, He^+, He^{q+} [9], He^{2+} [10,11], and Ne^{q+} [11] cover regions where large kinetic energies are released following removal of two or more target electrons corresponding to fragmentation under mutual Coulomb repulsion present within the doubly or multiple charged H_2O^{2+*} ions formed (Coulomb explosion). To the best knowledge of the authors, the only measurements of the distribution of the fragment energy release for electron impact are the measurements of Fremont *et al.* [12] at energies up to 200 eV.

Very recently, a comprehensive set of total cross section measurements of the uniquely defined dissociation pathways for ionization and electron capture collision processes by 15–100 and 500–3500 keV proton projectiles was reported through the use of coincidence counting techniques [13] and ionization collision processes by 30–1500 eV electron projectiles [14] using the pulsed beam—delayed target extraction experimental technique. In the present paper we extend the pulsed beam technique and incorporate the drift tube time-of-flight (TOF) based velocity measuring method to report measurements of energy releases of the H^+ fragments by protons at the impact energies of 20, 50, and 100 keV and by electrons at the impact energies of 35, 200, 400, and 1000 eV. Our measuring technique has allowed us to successfully cover a very large ejection energy region stretching from the very low 0.1 eV value to the high 30 eV value where the majority of the H^+ fragment ions are found.

*Corresponding author.

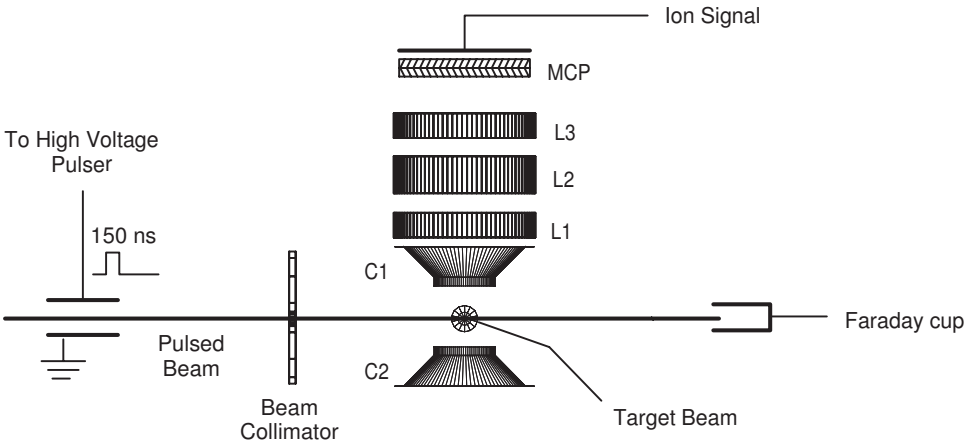

FIG. 1. Schematic diagram of the apparatus.

The present measurements are of direct practical relevance in modeling of the water loss from comet and planetary atmospheres and, as noted above, in chemistry in characterizing the radiolysis of liquid phase of water. Since the production of the H^+ fragment is accompanied with the highly reactive OH radical either as neutral or in its ionized form, these measurements will also find important uses in radiotherapy where water radicals are thought to provide 70% of the body cell death [1]; the proton data will find relevance in the now popular but expensive proton therapy and the electron data in the electron and x-ray based therapy. The measurements will also find important uses in the thermonuclear industry where the buildup of the H_2 and the O_2 gases from fragmentation of water by fission products affects the safety of the power plants and the corrosion of the fuel rods [15].

II. EXPERIMENTAL APPROACH

The energy distributions of the H^+ fragment ions released from the H_2O^{+*} and the H_2O^{2+*} dissociative precursor states formed during collisions with energetic projectiles were measured in the present work by a TOF based method on the apparatus shown in Fig. 1. Our previously measured total ionization, the total one electron capture cross sections by 15–100 and 500–3500 keV proton impact [13], and the total ionization cross sections by 30–1500 eV electron impact [14] suggest that formation of the triply charged H_2O^{3+*} precursor states will be negligible in the present study and are ignored from further discussions.

The main apparatus and the experimental procedure used have been described previously [16–18] and only the main features and minor modifications are summarized here. A beam of protons obtained from 10 to 100 kV ion accelerator of The Queen's University of Belfast and a beam of electrons obtained from an electron gun able to slide in and out of the ion beam path were arranged to cross a well collimated thermal energy beam of H_2O molecules 4 mm in diameter inside a high vacuum chamber at 90°. The projectile beam was collimated to 1 mm in diameter prior to entering the interaction region. The proton and the electron projectile beams were operated in a pulsed mode with a 150 ns wide beam pulses passing through the interaction region at a repetition rate of 10^4 Hz. The interaction region was surrounded by electrodes C1 and C2 with high transparency grids mounted at the apex to allow the ejected dissociation fragments to travel away from the interaction region. In the present study the ejected fragments were allowed to travel a distance of 42 mm before they were detected by a two microchannel plates based detector assembly. If required, a delayed extraction pulse immediately following the transit of the trailing edge of the incident beam pulse could be applied across the electrodes C1 and C2 to extract and detect all of the target ions formed. This was done from time to time to record the full mass spectrum of the target ion products and to verify that the target beam remained purely of water molecules throughout the measurements. The lens combination L1, L2, and L3 were used in this case to maximize the collection of all the target ions. During the energy distribution measurements L1, L2, and L3 were held at the ground potential along with the electrodes C1 and C2. The insides of the extraction and the lens electrode assemblies were all coated with a thin layer of graphite loaded resin to ensure that effects of contact potentials resulting from dissimilar materials used in the fabrication of the assemblies and a small amount of charging up of slightly oxide surfaces formed on exposure of the assembly electrodes to air were minimized to negligible values, thereby ensuring that the energy distribution measurements were carried out in a completely field-free region. Past experience has shown that such a precaution is necessary as these effects alter the energies and the trajectories of the ejected ions and falsify the measured energy values. A reference pulse obtained from the projectile beam pulser was used as a start pulse in the recording of the TOF spectra.

The measured TOF spectra were converted into energy spectra using a standard procedure [19] where the velocity component along the spectrometer axis is obtained from the measured flight time across the 42 mm distance to the detector. The energy resolution of the extracted spectra is dependent on the width and the pulse duration of the beam used in the measurement. Our solid angle is small enough (approximately 0.2 rad) to consider that essentially only on-axis fragments reach the detector. This assumption introduces an error of less than 4% in the extracted energy spectra from the variations in the flight times of ions arriving at the periphery of the detector in relation to the center. With the 1 mm wide beam and the pulse duration of 150 ns used in the present

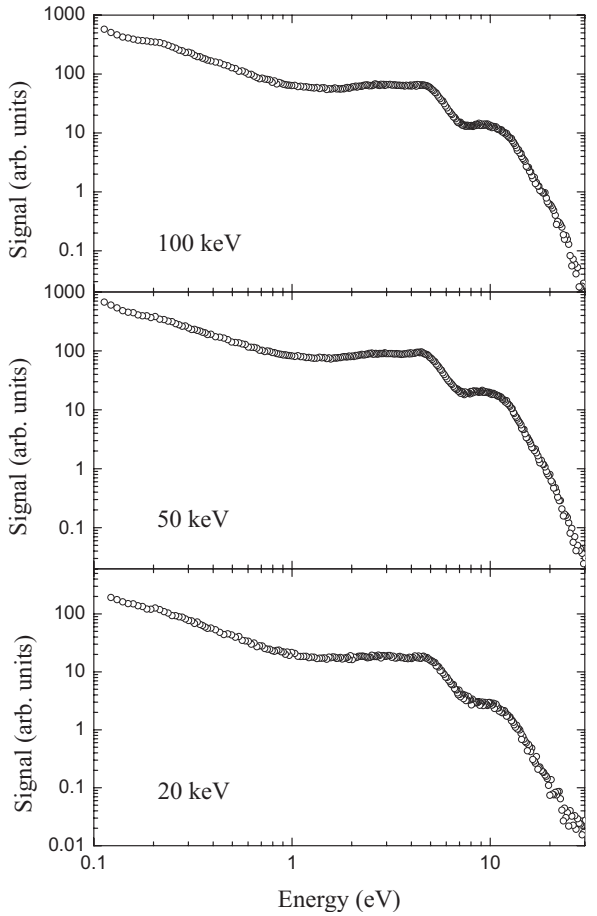

FIG. 2. Extracted energy distribution spectra of H^+ fragments emitted at 90° to the proton projectile beam at 20, 50, and 100 keV incident energies.

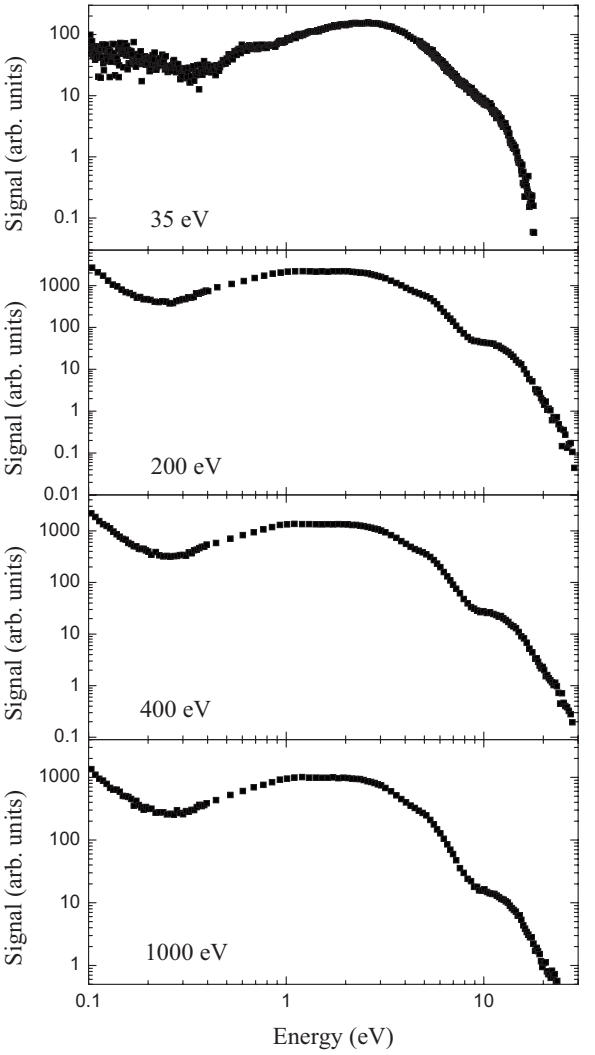

FIG. 3. Extracted energy distribution spectra of H^+ fragments emitted at 90° to the projectile beam direction for electrons at 35, 200, 400, and 1000 eV incident energies.

measurements, the combined uncertainties are around 6% for fragments that are ejected with an energy of 10 eV and around 3% for those ejected with an energy of 3 eV.

The target gas beam was formed inside a separately pumped nearby chamber by effusing water molecules through a bunch of 1 mm diameter hypodermic needles 10 mm in length bunched inside a 5 mm in diameter tube holder. The water reservoir supplying the molecules was filled with a high grade distilled water and was completely out-gassed by pumping the water for about half an hour prior to the experiment. The mass spectrum mentioned above showed that this procedure of removing absorbed air from the water was entirely satisfactory. Periodically measured mass spectra showed that leaking of outside air through the transport tube connecting the reservoir to the controlling needle valve was negligible.

III. ENERGY DISTRIBUTIONS OF H^+ EJECTED IONS

Energy spectra constructed from the measured TOF spectra of the H^+ fragments emitted at 90° are shown in Fig. 2 for the 20, 50, and 100 keV proton projectiles and in Fig. 3 for the 35, 200, 400, and 1000 eV electron projectiles. The spectra cover a wide energy range spanning from 0.1 to 30 eV and contain the majority of the fragment ions ejected. The constructed spectra correspond entirely to H^+ released ions without contaminations from the OH^+ and O^+ ions. This is because the H^+ fragments carry a 17/18 fraction of the total dissociation kinetic energy released (KER). This, together with the small mass, means that the H^+ fragment ions have a shorter TOF than the heavier ones in the measured TOF spectra. As an example, let us consider the worst scenario and inspect the spectra at the lowest energy of 0.1 eV where the likelihood of OH^+ and O^+ ion arrival will be the largest. For the OH^+ ions to arrive at the detector at the same time as the 0.1 eV H^+ ions, the energy of the OH^+ ions would need to be 1.7 eV. Further, as the OH^+ ions carry only 1/18 of the KER value released, the KER values in this case would need to be 30.6 eV. But collisions with 30.6 eV KER values should also give rise to the emissions of H^+ fragments with ejection energies of 28.9 eV. Figures 2 and 3 show that the spectra at 28.9 eV are negligibly small and confirm that even our lowest energy spectra at 0.1 eV are relatively free from any OH^+ and O^+ ion contributions.

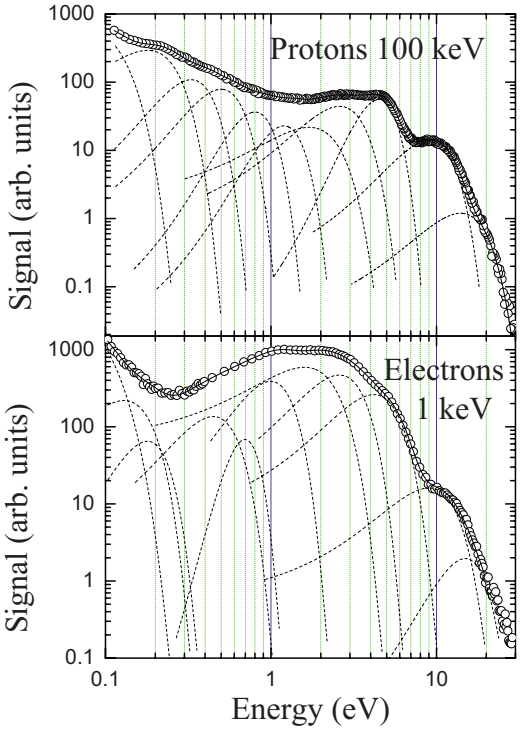

FIG. 4. (Color online) Least-squares fits to the extracted H^+ energy distribution spectra for 100 keV proton impact and 1000 eV electron impact using Gaussian peak profiles, which are included just to give some guidance in comparing both spectra. The scales on the ordinates are not related to one another.

It is apparent from Fig. 2 that the proton spectra at 20, 50, and 100 keV are remarkably similar in appearance with one another with all showing pronounced structures at around 4.5 and 9 eV fragment energies. Close inspection of 50 and 100 keV spectra reveals a presence of further peaks appearing at around 2 and 15 eV as very shallow structures. For electron projectiles, the spectra at 200, 400, and 1000 eV impact energies also show close similarities with one another with a pronounced peak appearing at around 9 eV fragment energy, shallow peaks at around 1, 3, and 4.5 eV, and one high energy peak around 15 eV (this peak is more apparent with the 1000 eV spectra). The 35 eV impact energy spectrum is a little different than the 200, 400, and 1000 eV spectra. It shows a much rapidly decreasing yield beyond the 9 eV peak, and in contrast to almost flat spectra between the 1 and 3 eV energy regions seen in the 200, 400, and 1000 eV spectra, the 35 eV spectrum shows instead a gradual rise to a maximum at around 3 eV. Although the statistics is poor, the 35 eV spectrum also shows the presence of a peak at around 0.6 eV not seen in the 200, 400, and 1000 eV spectra. As 35 eV electron projectiles are susceptible to greater threshold effects, it is perhaps not surprising to find that the spectra beyond 3 eV are considerably suppressed.

We have made an effort to fit our spectra using a least-squares fitting procedure with peaks having a Gaussian profile with the purpose to see, in a more quantitative way, if the spectra from proton and electron impact show some common pattern. Indeed, as seen in Fig. 4 for the selected cases of 100 keV protons and 1000 eV electrons, the yields beyond 3 eV are well reproduced by unique peaks for both projectiles. However, the region below 3 eV requires a collection of close lying peaks to reproduce the measurements. Because we found it difficult to extract the precise positions of the peaks below 3 eV, we place little faith in these peaks. They are only included to demonstrate that the region above 3 eV is dominated by well separated peaks and the region below 3 eV by many close lying peaks, which probably indicate a dissociation mechanism which gives a broad kinetic energy distribution for the H^+ fragments in this region.

The populating of the doubly-charged excited states requires the transfer of substantial amounts of energy in comparison with populating the singly-charged excited states. Thus, we can divide the present spectra into a "hard" collision region, associated with large ejection energies, and a "soft" collision region, associated with low ejection energies. It was also recently shown [14] in the case of the single and double ionizations of water molecules by 30–1500 eV electrons that at electron collision energies beyond 150 eV, the $H^+ + OH^+$ and the $H^+ + O^+$ ion pairs have a combined total cross section that is larger than 20% of the total H^+ formed from the sum of the single and the double ion pair productions. In that work the authors were unable to measure the cross sections for the $H^+ + H^+$ ion pair production so the total numbers of H^+ ions produced from the doubly excited H_2O^{2+*} states should be even higher than 20%. To account for this over 20% of the H^+ contribution to the total H^+ fragmentation coming from the H_2O^{2+*} states, inspection of Fig. 3 shows that the peak around the position of 4.5 eV must be taken to arise from the H_2O^{2+*} states in addition to the peaks around the 9 and the 15 eV energy regions. The present spectra can thus be classified as being hard for H^+ fragments having ejection energies larger than ~3 eV and as soft for H^+ fragments having ejection energy smaller than ~3 eV. Figures 2 and 3 show that the soft collision region is where the spectrum is described by many overlapping peaks.

Comparison of the proton spectra in Fig. 2 with those of the electron spectra in Fig. 3 reveals that the proton and the electron projectiles exhibit some very interesting deviations. First, the electron spectra beyond 4.0 eV fall off much faster with increasing ejection energy than do the proton spectra and second, below 4.0 eV, the electron spectra show the presence of a profound dip at around 0.25 eV which is completely absent in the proton spectra. The proton spectra, instead, show a monotonic rise with the decreasing ejection energy right down to the presently measured 0.1 eV energy value. These deviations indicate that there are important differences present in the collision dynamics between the two projectiles.

In a recent paper by Scully *et al.* [20] it was shown that at high electron collision energies the majority of the doubly excited H_2O^{2+*} states emanate from postcollision rearrangements following a removal of one of the $2a_1$ water orbital electrons during a single ionization collision event followed by a subsequent filling of the $2a_1$ vacancy through an Auger autoionization process ejecting a second electron from any one of the two outermost orbitals $1b_1$ or $3a_1$. The binding energies of the $1b_1$, $3a_1$, $1b_2$, and $2a_1$ orbitals are 12.60, 14.84, 18.78, and 32.62 eV, respectively [21]. The H_2O^{2+*} state can also be formed through two ionization processes

occurring ("two steps") during a single collision event, but it was shown in Ref. [20] that for electron projectiles this process is negligible in relation to the postcollision autoionization process. For electron projectiles, the hard collision region of the spectra, beyond 3 eV, can thus be attributed to single ionization events ("one step") removing a $2a_1$ orbital electron. Recent measurements of the KER [8] by electron impact corroborate this finding. The measured KER of 3.6 eV associated to ionic pair production is more likely to be energetically compatible with a single ionization followed by autoionization instead of a vertical Frank-Condon transition [8].

Two-step processes are fast and obey Franck-Condon straight line transition rules, so the doubly-charged precursor states formed during such collision events promote the states to very steep portions of their potential energy curves, thus involving large amounts of excitation energies. While electron projectiles have difficulties imparting such energies this is not the case with proton projectiles even at our lowest energy of 20 keV. The proton spectra are thus able to receive contributions from one-step processes (capture or ionization) as well as from two-step processes involving either transfer-ionization type collisions (capture plus ionization) or two ionizations during a single collision event. From Figs. 2 and 3 (and more clearly from Fig. 4), it can be seen that the proton-induced yields around the 4.5, 9, and 15 eV peaks are roughly of equal size, one order of magnitude smaller and two orders of magnitude smaller, respectively, than the spectra around the 2 eV region, while for the electron spectra, the similar figures are one order of magnitude smaller, two orders of magnitude smaller, and three orders of magnitude smaller, respectively. As protons and electrons carry a unity charge, the one-step collision processes are expected to be similar in size for both projectiles so that these much enhanced contributions to the proton spectra in the hard collision region must come from the two-step processes. Our set of carefully measured proton and electron energy spectra is thus able to provide a direct evidence of the importance of two-step processes present with proton projectiles. It should be noted that transfer-ionization and double capture processes for low-energy He^{2+} collisions with water also produce H^+ fragments with kinetic energies of ~6 and 15 eV [11], associated with the $H^+ + OH^+$ and $H^+ + O^+$ branches, respectively, in good agreement with our results, and indicating that these KERs are essentially independent of the removal mechanisms as long as the collision time is short when compared with the typical molecular vibration period.

Scully *et al.* [20] also showed that the ionization of a $1b_2$ orbital electron by electrons leads to branching to either the $OH + H^+$ ion or the $OH^+ + H$ ion pairs while the ionization of the $1b_1$ or the $3a_1$ orbital electron leads to the formation of a stable parent H_2O^+ ion. These orbital electrons require small amounts of energy transfer and the collisions involving these orbital electrons can be considered as being soft. One-step soft collision processes with protons would also involve the $1b_2$, $1b_1$, or $3a_1$ orbital electrons with the $1b_2$ removal leading to $OH + H^+$ ion or the $OH^+ + H$ ion pairs and the $1b_1$ or $3a_1$ removal leading to stable parent H_2O^+ ion formation. The soft region of the electron and the proton projectile energy spectra can thus be attributed to the ionization of a $1b_2$ orbital electron. The soft region contains the largest contributions to the total H^+ fragmentation yields for both the projectiles.

To our best knowledge, we are not aware of any previously measured proton-induced spectra of the H^+ fragments covering the present emission energy range. For electrons, we are aware of only one work, that of Fremont *et al.* [12], which covers a similar fragment energy region as the present one for a range of collision energies below 200 eV. The energies of the fragments in Ref. [12] were determined by the use of the electrostatic parallel plate method. Rather disturbingly, these measurements are completely at variance with ours. For instance, the positions of some of the peaks in Ref. [12] seem to change in position with incident energies. The Gaussian peaks fitted to our data, as illustrated in Fig. 4, were in part carried out to see if our spectra also contained such shifts in the peak positions with collision energy. Our fitting procedure showed that the extracted peaks in fact remained fixed in positions for the entire electron as well as the proton impact energies. There is also another cause for concern. The pronounced low-energy peak identified in Ref. [12] as *b* is absent in our measurements. We are not able to find reasons for such discrepancies between the two sets of measurements, one based on the TOF method and another on the parallel plate energy analysis method. One should note, however, that the parallel plate analysis methods only provide information about the energies of the ejected species and not their masses thus H^+, OH^+, and O^+ ions could all be recorded at a given energy setting if they happen to have the same energies. The TOF technique, on the other hand, measures only the velocity of the fragments and the time window used in our measurements, as mentioned before, only allowed the recording of the faster moving light H^+ ions.

IV. CONCLUSIONS

We have carried out energy distribution measurements of the H^+ fragment ions emitted by proton and electron projectiles from water. The energy spectra are shown to contain negligible contaminations from the OH^+ and O^+ fragment components. The spectra are divided into the soft collision region containing H^+ fragments with ejection energies ≤ 3 eV and the hard collision region containing ejection energies ≥ 3 eV. The high statistics of our spectra is able to show that the extended broad spectra in the soft region contain many shallow structures which curve fitting procedures have identified as belonging to many overlapping peaks. The hard region also contains many peaks but these are all well resolved.

The soft region is shown to be populated by singly-charged H_2O^{+*} excited precursor states, while the hard region is shown to be populated by the doubly-charged H_2O^{2+*} excited precursor states. For electrons the soft and the hard regions both involve one-step collision events; in the later case the removal of a $2a_1$ orbital electron and postcollision autoionization dominates. For protons added contributions from two-step collision events are present as well and these are shown to be responsible for the presence of substantially enhanced contributions in the hard collision region. The elec-

tron spectra exhibit a pronounced dip around 0.25 eV ejection energy which is completely absent with protons. The reason for this observed difference is unclear. However, it should be emphasized that these differences in the H^+ energy spectra between protons and electrons are not the only differences concerning the H^+ emission. The overall effect of the capture channels is expected to provide added contributions in the soft part of the H^+ spectra. The energy balance for removing a $1b_2$ or a $2a_1$ orbital electron, responsible for the H^+ fragment emissions, is much smaller in capture than in ionization collisions by an amount equal to the internal energy of the H^+ projectile (13.6 eV). But there are also differences in the ionization channels. For decreasing velocities from $v<2$ a.u. (i.e., $E<100$ keV for protons and $E<55$ eV for electrons) the H^+ production cross section from the ionization channel for proton impact shows a clear increase as the projectile velocity decreases [13], while the electron impact cross sections show the opposite behavior [7,8,14]. The reason for this increase in the H^+ production with protons can be attributed to the inhibition for the ionization channel to remove $1b_1$ and $3a_1$ electrons due to the competition with electron capture [13], thus giving a relative enhancement, with respect to electron impact, in removing electrons from the $1b_2$ and $2a_1$ orbitals which gives rise to the H^+ production. These low-energy ionizing collisions favor small energy transfers which might result in H^+ emission with small KER.

It should be pointed out that Figs. 2–4 are plotted on a log-log scale and thus give artificially enhanced importance to spectra at low emission energies. In reality, the majority of the fragments are contained within the energy range of up to 4 eV for both the electron and the proton projectiles. The total ionization cross sections are thus dominated by one-step collision processes and so they can rarely be used to highlight differences in the proton and the electron collision mechanisms. However, as we show, the proton and electron impact energy spectra do contain large observable differences. They are thus an important tool for examining direct evidences of differences in collision dynamics of the protons and the electrons.

ACKNOWLEDGMENTS

The authors would like to thank the Brazilian Agencies CAPES and CNPq for providing funds to A.L.F.d.B. and H.L. M.B.S. and J.L. would like to acknowledge financial assistance from the EPSRC (UK). E.C.M. acknowledges financial support from Brazilian Agencies CNPq and FAPERJ.

[1] E. J. Hall, *Radiobiology for the Radiologist*, 5th ed. (Lippincott, Philadelphia, PA, 2000).
[2] B. C. Garrett *et al.*, Chem. Rev. (Washington, D.C.) **105**, 355 (2005).
[3] F. Gobet, B. Farizon, M. Farizon, M. J. Gaillard, M. Carre, M. Lezius, P. Scheier, and T. D. Mark, Phys. Rev. Lett. **86**, 3751 (2001).
[4] U. Werner, K. Beckord, J. Becker, and H. O. Lutz, Phys. Rev. Lett. **74**, 1962 (1995).
[5] P. M. Y. Garcia, G. M. Sigaud, H. Luna, A. C. F. Santos, E. C. Montenegro, and M. B. Shah, Phys. Rev. A **77**, 052708 (2008).
[6] H. Luna and E. C. Montenegro, Phys. Rev. Lett. **94**, 043201 (2005).
[7] H. C. Straub, B. G. Lindsay, K. A. Smith, and R. F. Stebbings, J. Chem. Phys. **108**, 109 (1998).
[8] S. J. King and S. D. Price, Int. J. Mass Spectrom. **277**, 84 (2008).
[9] F. Alvarado, R. Hoekstra, and T. Schlatholter, J. Phys. B **38**, 4085 (2005).
[10] B. Seredyuk, R. W. McCullough, H. Tawara, H. B. Gilbody, D. Bodewits, R. Hoekstra, A. G. G. M. Tielens, P. Sobocinski, D. Pesic, R. Hellhammer, B. Sulik, N. Stolterfoht, O. Abu-Haija, and E. Y. Kamber, Phys. Rev. A **71**, 022705 (2005).
[11] P. Sobocinski, Z. D. Pesic, R. Hellhammer, D. Klein, B. Sulik, Y. D. Chesnel, and N. Stolterfoht, J. Phys. B **39**, 927 (2006).
[12] F. Fremont, C. Leclercq, A. Hajaji, A. Naja, P. Lemennais, S. Boulbain, V. Broquin, and J. Y. Chesnel, Phys. Rev. A **72**, 042702 (2005).
[13] H. Luna, A. L. F. de Barros, J. A. Wyer, S. W. J. Scully, J. Lecointre, P. M. Y. Garcia, G. M. Sigaud, A. C. F. Santos, V. Senthil, M. B. Shah, C. J. Latimer, and E. C. Montenegro, Phys. Rev. A **75**, 042711 (2007).
[14] E. C. Montenegro, S. W. J. Scully, J. A. Wyer, V. Senthil, and M. B. Shah, J. Electron Spectrosc. Relat. Phenom. **155**, 81 (2007).
[15] D. R. Olander, Y. S. Kim, W. E. Wang, and J. Yagnik, J. Nucl. Mater. **270**, 11 (1999).
[16] H. Luna, M. Michael, M. B. Shah, R. E. Johnson, C. J. Latimer, and J. W. McConkey, J. Geophys. Res. **108**, 5033 (2003).
[17] H. Luna, C. McGrath, M. B. Shah, R. E. Johnson, M. Liu, C. J. Latimer, and E. C. Montenegro, Astrophys. J. **628**, 1086 (2005).
[18] C. McGrath, M. B. Shah, P. C. E. McCartney, and J. W. McConkey, Phys. Rev. A **64**, 062712 (2001).
[19] D. J. Auerbach, in *Atomic and Molecular Beam Methods*, edited by G. Scoles (Oxford University Press, New York, 1988), Vol. 1, p. 365.
[20] S. W. J. Scully, J. A. Wyer, V. Senthil, M. B. Shah, and E. C. Montenegro, Phys. Rev. A **73**, 040701(R) (2006).
[21] B. Winter, R. Weber, W. Widdra, M. Dittmar, M. Faubel, and I. V. Hertel, J. Phys. Chem. A **108**, 2625 (2004).